Wetting in a two-dimensional random-bond Ising model

Ming Huang

Laboratory of Atomic and Solid State Physics, Cornell University, Ithaca, New York 14853

Michael E. Fisher

Institute for Physical Science and Technology, University of Maryland, College Park, Maryland 20742

Reinhard Lipowsky

Institut für Festkörperforschung, KFA Jülich, Postfach 1913, D-5170 Jülich, Federal Republic of Germany

(Received 6 July 1988)

We analyze a square-lattice random-bond Ising model using a numerical transfer-matrix technique to test the theory proposed by Lipowsky and Fisher for the complete wetting transition of a wall by one of two phases which coexist in a random medium. The theoretical scaling arguments are checked in detail. The transverse and longitudinal correlation lengths, $\xi_\perp(h)$ and $\xi_\parallel(h)$, are found to be related by $\xi_\perp \sim \xi_\parallel^\zeta$ with $\zeta = 0.65 \pm 0.02$ as the external field, or chemical potential deviation, h, approaches 0: the theoretical expectation is $\zeta = \frac{2}{3}$. The mean wetting layer thickness diverges as $\bar{l}(h) \sim h^{-\psi}$ while $\xi_\perp \sim h^{-\nu_\perp}$ as $h \to 0$ with $\psi = \nu_\perp = \frac{1}{2}$.

I. INTRODUCTION

Interfacial wetting phenomena in random systems have been studied recently by Lipowsky and Fisher.[1,2] On the basis of scaling arguments, various types of universal behavior were predicted for the singularities arising at complete and critical wetting transitions. The aim of the work reported here is to test and explore aspects of this theory by explicit numerical calculations for a two-dimensional random-lattice model which exhibits a complete wetting transition in which an interface bound to a wall delocalizes as the external field or chemical potential is varied. To provide the necessary background, a brief outline of the relevant scaling theory is presented first.

Consider two phases, α and β, which may coexist in a random medium which is bounded by an inert third phase which we will regard as a rigid, solid planar wall. If the interactions are such that phase β is favored by the wall, the bulk phase α may be separated from the boundary by a wetting layer of phase β. The mean-layer thickness $\bar{l}(T,h)$ may diverge continuously to ∞ in response to changes in the temperature T or in the field h which represents the deviation from bulk $\alpha\beta$ coexistence as, say, the chemical potential difference $\Delta\mu$ (which is positive on the α side of the bulk equilibrium phase boundary). If $\bar{l} \to \infty$ as $h \to 0$ for fixed T one has *complete wetting*. (More precisely, if $\bar{l} \to \infty$ for T in an open interval around a fixed value one has complete wetting; at a *critical wetting point*[2] T_{cW}, the layer thickness remains finite as $h \to 0$ when T is on one side, generally the lower side, of T_{cW}.) The divergence of $\bar{l}$ may be characterized generally by the power law

$$\bar{l}(T,h) \sim 1/h^\psi \quad \text{as} \quad h \to 0+ . \tag{1}$$

Impurities which are quenched in a medium give rise to an inhomogeneous random potential $V_R(\mathbf{x},z)$ which

may be regarded as acting on the *interface* separating the α and β phases. Here we denote coordinates parallel to the $(d-1)$-dimensional boundary by $\mathbf{x}$, while z denotes the orthogonal coordinate normal to the wall with origin on the wall. At nonzero T the interface will wander under the influence of thermal fluctuations. In the presence of a random potential it will wander even at $T=0$ in an endeavor to find the configuration of lowest energy. This effect alone, in the absence of any walls or boundaries, can (for $h=0$) be characterized by a single *roughness* or *wandering* exponent[2-7] ζ: The typical transverse excursion $L_\perp$, normal to the mean plane of the interface, over a longitudinal scale $L_\parallel$ varies as

$$L_\perp \sim L_\parallel^\zeta . \tag{2}$$

If the wandering exponent retains its significance in the presence of a wall and a bulk field h, scaling implies[1,2] the relation

$$\xi_\perp(h) \equiv \langle (l - \langle l \rangle)^2 \rangle^{1/2} \sim [\xi_\parallel(h)]^\zeta , \tag{3}$$

where $\xi_\parallel(h)$ is the longitudinal correlation length which describes the decay of the correlation function

$$C(\mathbf{x}) \equiv \langle l(\mathbf{x})l(0) \rangle - \langle l(\mathbf{x}) \rangle \langle l(0) \rangle , \tag{4}$$

in which $l(\mathbf{x})$ is the local interface thickness. (The precise definition of the expectation value $\langle \cdots \rangle$ will be given below.) When the interactions between the constituent molecules, etc., in the three phases are of short range, or decay sufficiently rapidly,[1,2] any effective long-range force between interface and wall may be neglected. In these circumstances one is typically in a *weak-fluctuation* regime (as against a mean-field regime[1,2]) and one anticipates[1,2]

$$\bar{l} \sim \xi_\perp . \tag{5}$$

The total effective Hamiltonian for the interface may be taken as

$$\mathcal{H}\{l(\mathbf{x})\} = \int d^{d-1}x [\Sigma_0 + \tfrac{1}{2}\bar{\Sigma}(\nabla l)^2 + hl + V_R(\mathbf{x},l)] , \quad (6)$$

where Σ_0 is the interfacial tension while $\bar{\Sigma}$ is the interfacial stiffness; these parameters may be regarded as fixed here.

The basic scaling relation follows by focusing on the interface in a typical realization of the randomness and arguing that it wanders through a transverse displacement $\xi_\perp$ over regions of longitudinal dimensions $\xi_\parallel$. Thus the gradient term in (6) can be estimated by

$$\tfrac{1}{2}\bar{\Sigma}(\nabla l)^2 \sim \bar{\Sigma}(\xi_\perp/\xi_\parallel)^2 \sim \xi_\parallel^{-2(1-\zeta)/\zeta} . \quad (7)$$

When h vanishes the balance between this gradient term, which tends to make the interface flat and the random-interaction term, can be expected to result in the contribution to the free energy due to $V_R(\mathbf{x},l)$ being of essentially the same magnitude. Finally, on including the field term in (6), the total free energy per unit $(d-1)$-dimensional area of the interface should be well represented by

$$f \approx h\bar{l} + A\xi_\perp^{-2(1-\zeta)/\zeta} , \quad (8)$$

where A is a constant. Using (5) and minimizing this expression yields (1) with[1]

$$\psi = \nu_\perp = \frac{\zeta}{2-\zeta} , \quad (9)$$

where $\nu_\perp$ is the, in principle independent, exponent for the divergence of $\xi_\perp$.

For a two-dimensional "random-bond" system,[2] in which the random potential tends to pin the interface but does otherwise not distinguish between phases α and β, one knows[6,7] that $\zeta = \tfrac{2}{3}$. Thus a complete wetting transition of a one-dimensional interface in a two-dimensional random-coupling medium should have $\psi = \tfrac{1}{2}$. This prediction and relations (3) and (5) will be tested by our calculations, described below, for the square-lattice random-bond Ising model at $T=0$.

II. LATTICE MODEL

The model we have employed is adapted from that developed by Huse and Henley in their pioneering paper.[6] It may be regarded as a semi-infinite square-lattice Ising model confined to $z > 0$ with random couplings between nearest-neighbor spins. A variable uniform bulk field h is applied in the "up" direction to favor the bulk, spin-up, α phase, while a fixed, strong local magnetic field in the "down" direction is applied at the boundary to favor the spin-down or β phase for spins close to the boundary. Explicitly we suppose that the closest layer of spins to the wall is fixed to be down under the influence of the local field. The effect of the random-bond impurities is assumed sufficiently weak so that the system still orders ferromagnetically to form domains. Away from the bulk critical point, bubbles and overhangs can be ignored asymptotically.[8] Thus, as illustrated in Fig. 1, a one-dimensional interface represented by a single-valued
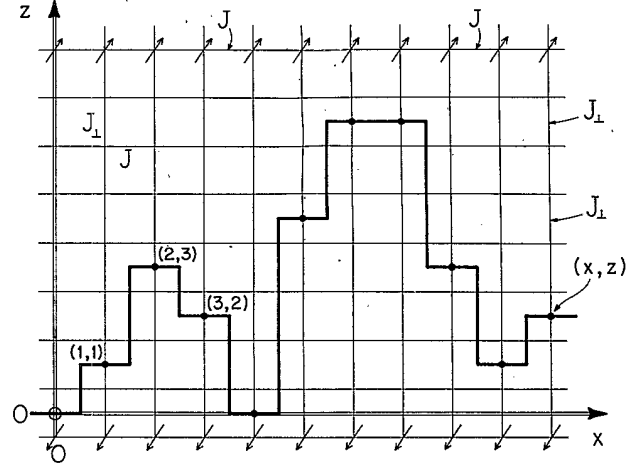

FIG. 1. Illustration of an interface or path lying on the dual of a lattice of Ising spins at $T=0$ and separating a bulk domain of up spins from a wetting layer of down spins in contact with a wall forming the lower edge of the lattice. Horizontal bonds of fixed strength J are intersected by vertical sections of the path; vertical bonds of strength $J_\perp$, distributed uniformly in an interval $(-\sqrt{3}, +\sqrt{3})\Delta J$, are cut by the horizontal segments of the path. The integer coordinates (x,z) of the path $z=l(x)$ are taken to lie on the vertical Ising bonds.

function $z(x)$, which separates the two domains of up and down spins, can be used to account for all the degrees of freedom of the system. For simplicity of language we will regard the system as at zero temperature, $T=0$; however, since the thermal fluctuations are found to be technically irrelevant,[6] the singular behavior discovered should apply equally for all $T < T_c$.

In a particular realization of the randomness and for a given configuration of the interface, the total energy can be calculated simply by regarding the interface as breaking the bonds it crosses (see Fig. 1). Horizontal or parallel bonds of strength $J_\parallel$ are intersected by vertical segments of the path of the interface while vertical or perpendicular bonds of strength $J_\perp$ are cut by horizontal segments of the path. The total interface Hamiltonian can thus be written

$$\mathcal{H}\{z(x)\} = \sum_x [\bar{J}_\parallel(x,z(x;x+1))|z(x+1)-z(x)|$$
$$+ J_\perp(x,z(x)) + Hz(x)] , \quad (10)$$

where $\bar{J}_\parallel(x,z(x;x+1))$ represents the average strength of the horizontal bonds crossed by the path $z(x)$ between x and $x+1$, while H denotes the bulk magnetic field and x and z are measured in units of the lattice spacing. At $T=0$ the problem reduces to finding the configuration of lowest energy for a particular realization of random bonds, i.e., to an optimal path problem.[6] An average over realizations of the randomness is then called for.

The anticipated universal singular behavior should not be sensitive to details of the randomness: in particular, randomness or lack thereof in the horizontal bonds should not change the asymptotic forms.[6] Accordingly, following Huse and Henley we take $\bar{J}_\parallel \equiv J$ to be constant.

On the other hand, we suppose that the vertical bonds are random with $J_\perp$ distributed uniformly in a range of width ΔJ_0, with no correlation from one bond location, (x,z) to another. Thus we have

$$\Delta J \equiv \langle (J_\perp - \langle J_\perp \rangle)^2 \rangle^{1/2} = \frac{\Delta J_0}{2\sqrt{3}} \ , \qquad (11)$$

where $\langle \cdots \rangle$ denotes an average over the random-bond distribution. A moment's reflection shows that the mean value $\langle J_\perp \rangle$ can play no significant role. In most of our calculations we have used the range $\Delta J_0 = 4\sqrt{3}J$ or, equivalently, $\Delta J = 2J$. This is the value adopted by Huse and Henley;[6] it is sufficiently large that one is not troubled by the crossover to a flat (or thermal) interface that arises when $\Delta J/J \to 0$ but is not so large that the path is displaced vertically by many lattice spacings on each step.

Now let $E(x_1,z_1;x_2,z_2)$ be the ground-state energy for all interfaces running from (x_1,z_1) to (x_2,z_2). For any x between x_1 and x_2 we evidently have

$$E(x_1,z_1;x_2,z_2) = \min_z [E(x_1,z_1;x,z) + E(x,z;x_2,z_2)] \ . \qquad (12)$$

This relation provides the basis for a transfer-matrix technique for calculating numerically the optimal path and its energy. The approach was devised originally by Derrida and Vannimenus.[9] We have employed the efficient procedure developed by Huse and Henley;[6] the algorithm was not described in their paper but is explained in the Appendix here.

For a fixed starting point, say $(0,z_0)$, and a given realization of random bonds ω, the method iteratively generates the sets of energies $E_\omega(0,z_0;1,z)$, $E_\omega(0,z_0;2,z)$, $\ldots$, $E_\omega(0,z_0;x,z)$ and the corresponding optimal paths from $(0,z_0)$ to (x,z). In practice, at each step of iteration a new column of random bonds of height Δz is chosen. The height of lattice explored, Δz, is chosen large enough to avoid finite-size limitations. We used the pseudorandom number generator $RAN1$ of Press et al.[10] Extensive tests of this generator were performed to check the required lack of correlation between neighboring and further-neighbor assignments of the bond couplings $J_\perp$. The results were very satisfactory with no detectable systematic effects.

For a fixed choice of parameters, initial height $l_0 \equiv z_0$, $x_{max} \equiv L_\parallel$, which ranged up to 1000, and external field

$$h = H/J \ , \qquad (13)$$

we ran N_ω distinct realizations. Typically $N_\omega = 3000$–7000 provided satisfactory statistics and well-determined mean values, computed from

$$\langle \cdot \rangle \equiv N_\omega^{-1} \sum_\omega \cdot \ . \qquad (14)$$

In the main the starting height was set at $l_0 = 0$. The overall optimal path or interface, $l_\omega(h;x,L_\parallel)$ for $0 \le x \le L_\parallel$, is then defined by the values of $z_\omega(x)$ for the path to $x = L_\parallel$ of lowest energy, $E_\omega(0,0;L_\parallel,z)$. Two typical graphs of $l_\omega(h;x,L_\parallel)$ are shown in Fig. 2. The *mean*
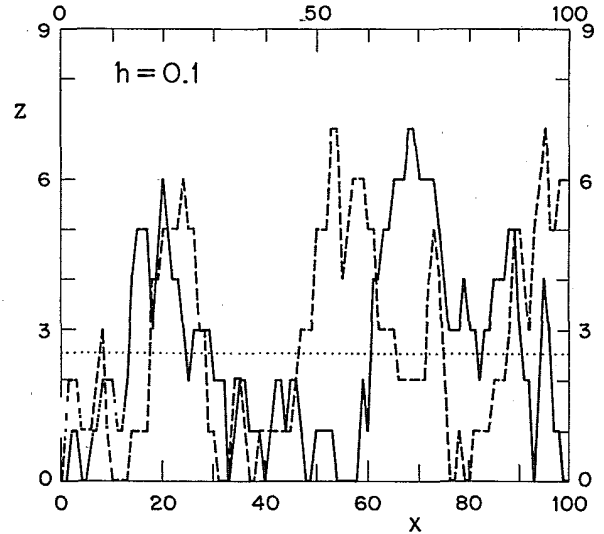

FIG. 2. Two examples (solid and dashed lines) of optimal paths or interfaces $l_\omega(h;x,L_\parallel)$ with $h = 0.1$ and $L_\parallel = 100$ in different realizations of the randomness with $\Delta J/J = 2$. The dotted line indicates the mean-layer thickness $\bar{l}(h)$ as estimated from 6000 realizations with $L_\parallel = 300$.

interface is defined by

$$l_{av}(h;x,L_\parallel) \equiv \langle l_\omega(h;x,L_\parallel) \rangle_\omega \qquad (15)$$

and, ideally, varies smoothly with x. Figure 3 illustrates a mean interface for $h = 0.01$ and $L_\parallel = 900$; evidently the residual statistical noise is quite small. In addition to the
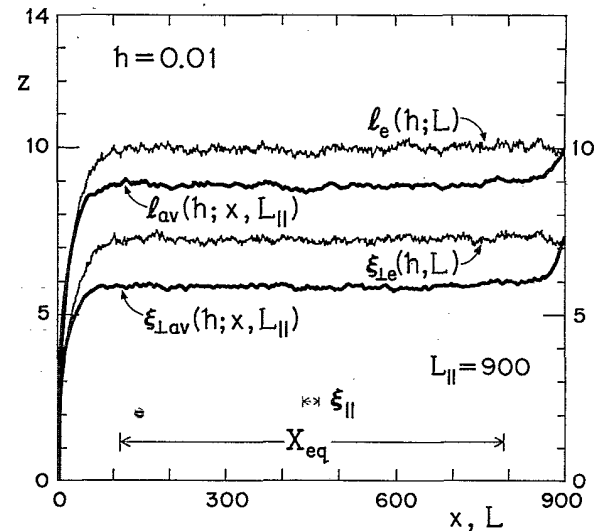

FIG. 3. Mean optimal path $l_{av}(h;x,L_\parallel)$ and corresponding transverse correlation length $\xi_{\perp av}(h;x,L_\parallel)$ (bold curves) for $h = 0.01$, $L_\parallel = 900$, and $\Delta J/J = 2$ as estimated from $N_\omega = 4000$ realizations. The light curves represent the corresponding endpoint trajectories $l_e(h;L)$ and $\xi_{\perp e}(h,L)$. Also indicated is the equilibrium range X_{eq} and the longitudinal correlation length $\xi_\parallel$ (see Sec. III).

mean path of the interface itself, it is useful, following the scaling theory, to define and compute the corresponding transverse fluctuation or correlation length

$$\xi_{1\mathrm{av}}(h;x,L_{\parallel})\equiv\langle[l_{\omega}(h;x,L_{\parallel})-\langle l_{\omega}(h;x,L_{\parallel})\rangle_{\omega}]^2\rangle_{\omega}^{1/2} .$$

(16)

This is also displayed in Fig. 3: it follows a similar course to $l_{\mathrm{av}}(x)$ but is smaller in magnitude.

One notices from Fig. 3 that around both ends, within a region that evidently must be comparable to $\xi_{\parallel}$, the longitudinal correlation length, the interface deviates from its apparent limiting ($L_{\parallel}\to\infty$) equilibrium level, $\bar{l}(h)$. The starting part near (0,0) can be understood easily as the relaxation from the initial condition $l_0=0$ up to the equilibrium level. The reason for the unexpected upwards deviation at the end near $x=L_{\parallel}$ is somewhat more subtle; but it is worth discussing here because of the light it throws on the interplay between the gradient, field, and random terms in the effective Hamiltonian (6) or, equivalently, between the corresponding terms, with coefficients $J_{\parallel}=J$, J_{1}, and H, in the model Hamiltonian (10).

Accordingly, let us first define X_{eq} as the interval $(k\xi_{\parallel},\ L_{\parallel}-k\xi_{\parallel})$, where k is chosen sufficiently large, say $k=5-8$, so that $l_{\mathrm{av}}(x)$ achieves, within the statistical noise level, the asymptotic equilibrium value $\bar{l}(h)$ (see Fig. 3 where both $\xi_{\parallel}$ and X_{eq} are indicated). (A precise definition of $\xi_{\parallel}$ is given below.) The equilibrium level depends, for fixed J and ΔJ, only on the field h and results from a balance between the random potential characterized by ΔJ and the gradient term corresponding to J. In a given realization, ω, in regions where the fluctuations in J_{1} are small the interface will stay flat, to reduce the tension, and low down, i.e., close to the wall, to reduce the bulk-field energy. However, if the J_{1} bonds are particularly weak in a region away from the boundary, the interface tends to deviate upwards in order to save energy by crossing weaker bonds. However, if it stays away from the boundary it starts to pay, on average, an increased cost in bulk-field energy, accordingly it soon falls back towards the wall. Thus, as can be seen from the examples in Fig. 2, a typical interface repeatedly bounces off the boundary in its search for the minimum energy path. It cannot stay too low since the presence of the boundary restricts the choice of accessible favorable random bonds. For $z=\bar{l}(h)$ fluctuations up and down balance in the long run.

How does this description break down near the end of the path at $x=L_{\parallel}$? As indicated, the interface will tend to rise above $\bar{l}(h)$ in order to sample a wider range of random bonds: there is a *local* cost in field energy although that sacrifice may be well worthwhile; but for x in X_{eq}, extra bulk-field energy would have to be paid later unless the wall soon fluctuates downwards. Near the end of the path, however, the interface does not have to worry about this delayed cost since it never proceeds beyond $x=L_{\parallel}$ to learn that it is now above $\bar{l}(h)$. In sum, then, it pays the interface, on average, to rise upwards at the end of the path as is observed.

The same arguments apply to the increase observed in

the fluctuation $\xi_{1}(h;x,L_{\parallel})$ at the end of the range. It is actually instructive to study two further, easily computed quantities which pertain directly to the end points of the optimal path, namely,

$$l_e(h;L)\equiv\langle l_{\omega}(h;L,L)\rangle_{\omega}$$

(17)

and

$$\xi_{1e}(h;L)\equiv\langle\xi_{1\omega}(h;L,L)\rangle_{\omega} .$$

(18)

Computed versions of these endpoint trajectories for the case of $h=0.01$ and $\Delta J/J=2$ are also shown in Fig. 3. Evidently, they display no final upturn; rather, for $L>\xi_{\parallel}$ they rapidly attain asymptotic equilibrium values $\bar{l}_e(h)$ and $\bar{\xi}_{1e}$. By scaling, both these values should diverge like $h^{-\psi_e}$ with $\psi_e=\psi=\frac{1}{2}$ as $h\to0$. Likewise the ratios $\bar{l}_e(h)/\bar{l}(h)$, $\bar{\xi}_{1e}(h)/\xi_{1}(h)$, and $\bar{l}(h)/\xi_{1}(h)$ should approach universal values when $h\to0$. These expectations have been tested as described below.

III. QUANTITATIVE ANALYSIS

The equilibrium interval $X_{\mathrm{eq}}\equiv(k\xi_{\parallel},\ L_{\parallel}-k\xi_{\parallel})$ described above (with $k=5-8$) provides estimates for the limiting wetting layer thickness and transverse correlation length via

$$\bar{l}(h)\cong\langle l_{\mathrm{av}}(h;x,L_{\parallel})\rangle_{\mathrm{eq}} ,$$

(19)

$$\xi_{1}(h)\cong\langle\xi_{1}(h;x,L_{\parallel})\rangle_{\mathrm{eq}} ,$$

(20)

in which $\langle\cdot\rangle_{\mathrm{eq}}$ denotes an average over all x in X_{eq}. For sufficiently large $L_{\parallel}$ (and fixed $\Delta J/J$) the results depend only on h. The limiting endpoint values $\bar{l}_e(h)$ and $\bar{\xi}_{1e}(h)$ are estimated similarly. The statistical uncertainties attached to the mean-data values were generally of "one-sigma" magnitude 0.3 to 2 %. They were estimated by treating data lumped over disjoint intervals within X_{eq} of length $2\xi_{\parallel}$ as independent, by dividing the N_{ω} (≥3000) realizations into groups of ten taken as independent and by evaluating the expression

$$\xi_{1}/[N_{\omega}(L_{\parallel}-2k\xi_{\parallel})/2\xi_{\parallel}]^{1/2} ;$$

these different routes gave quite similar results.

The results for $\bar{l}(h)$, etc., over a range of two to three decades in h from 0.1 to 0.0001 are shown on a log-log plot in Fig. 4. As indicated, scaling predicts that the asymptotic forms,

$$\bar{l}(h)\approx B/h^{\psi}, \qquad \bar{l}_e\approx B_e/h^{\psi} ,$$

(21)

$$\xi_{1}(h)\approx B_{1}/h^{\nu_{1}}, \qquad \bar{\xi}_{1e}(h)\approx B_{1e}/h^{\nu_{1}}$$

(22)

will be obeyed with $\psi=\nu_{1}=\frac{1}{2}$. The solid lines shown in Fig. 4 are drawn with a slope corresponding to the expected exponents. The data for $\bar{\xi}_{1e}(h)$ follow the line rather closely. The other plots, especially for $\bar{l}_e(h)$, show noticeable deviations for lower values of h; however, if one plots $\bar{l}_e(h)+\frac{1}{2}$ in place of $\bar{l}_e(h)$, which amounts only to a half-lattice spacing change in the definition of the layer thickness, then the points fall, within graphical accuracy, *on* the uppermost line in Fig. 4.

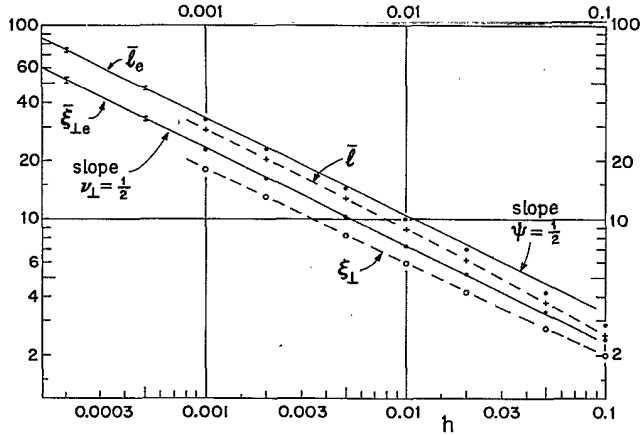In order to estimate the true asymptotic exponents for

FIG. 4. Logarithmic plots of layer thicknesses $\bar{l}(h)$, $\bar{l}_e(h)$, and transverse correlation lengths $\bar{\xi}_\perp(h)$ and $\bar{\xi}_{\perp e}(h)$ vs the field h for $\Delta J/J = 2$. The solid lines have slopes of $\frac{1}{2}$. Note that plotting $(\bar{l}_e + \frac{1}{2})$ in place of $\bar{l}_e$ brings the points essentially into coincidence with the upper line; the plot of $(\bar{l} + \frac{1}{2})$ is, similarly, closely linear (see text).

$\bar{l}(h)$, etc., more systematically, we have computed the slopes on the log-log plot of successive segments $(h_a h_b)$ of the data. The results are plotted in Fig. 5 versus $\bar{h}^{1/2}$, which is defined precisely in the caption and seems a reasonable candidate for the form of the leading correction to the power laws (21) and (22). The symbols and
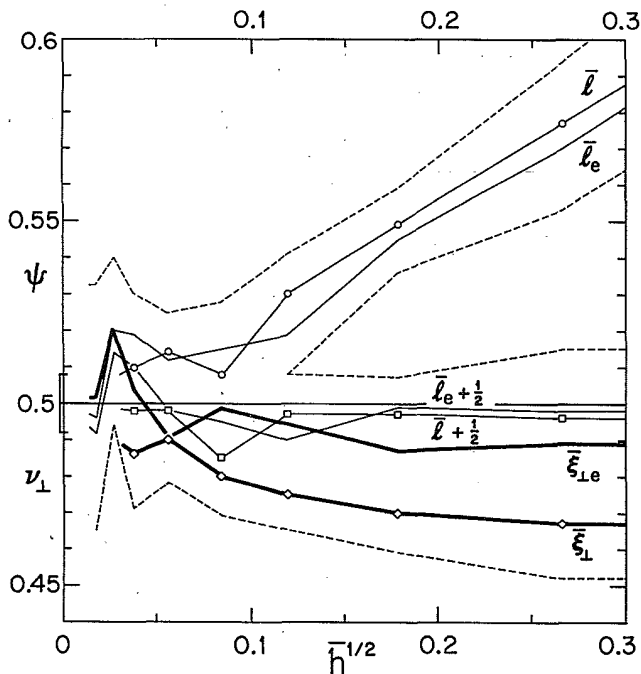

FIG. 5. Estimates of the exponent ψ (thin lines) and of $\nu_\perp$ (bold lines) derived from the segmental slopes of logarithmic plots of $\bar{l}(h)$, $\bar{l}(h) + \frac{1}{2}$, and $\bar{\xi}_\perp$ (lines with open symbols) and $\bar{l}_e$, $\bar{l}_e + \frac{1}{2}$, and $\bar{\xi}_{\perp e}$ (plain lines) over intervals (h_j, h_{j+1}). The dashed lines indicated the outer uncertainty limits of the individual slopes which are plotted vs $\bar{h}_j^{1/2} \equiv (h_j h_{j+1})^{1/4}$. As indicated on the left, the data suggest $\psi = \nu_\perp = 0.500 \pm 0.008$.

solid connecting lines represent the central estimates; the statistical uncertainties are encompassed by the dashed-line envelope. This figure clearly suggests a common exponent for all four functions and leads to the estimate

$$\psi = \nu_\perp = 0.500 \pm 0.008 , \tag{23}$$

corresponding to the uncertainty bar on the left side of the figure. The results are in full accord with the theory.

If one accepts the values $\psi = \nu_\perp = \frac{1}{2}$ the asymptotic amplitudes in (21) and (22) may be estimated in a similar way. In units of the lattice spacing, a, we find, for $\Delta J/J = 2$,

$$B = 0.932 \pm 0.005, \quad B_e = 1.049 \pm 0.005$$
$$B_\perp = 0.566 \pm 0.006, \quad B_{\perp e} = 0.720 \pm 0.010 . \tag{24}$$

The corresponding amplitude ratios, which should be universal, i.e., independent of $\Delta J/J$ (>0), follow from these results or, somewhat more reliably, can be estimated directly. Our preferred estimates are

$$\frac{B_e}{B} = 1.123 \pm 0.004, \quad \frac{B_{\perp e}}{B_\perp} = 1.267 \pm 0.006 ,$$
$$B_e/B_{\perp e} = 1.458 \pm 0.008 . \tag{25}$$

If one combines the scaling expression (8) for the free-energy density with (21) and (22) one is led to

$$\Delta \Sigma(h) = \Sigma(h) - \Sigma(0) \approx \bar{A} h^{2-\alpha} , \tag{26}$$

with $2 - \alpha = 1 - \psi = \frac{1}{2}$, where $\Sigma(h)$ is the overall interfacial tension or free energy per unit length parallel to the x axis. The equilibrium energy or ($T = 0$) tension is easily calculated from the data for x in X_{eq}. It is plotted in Fig. 6 against $h^{1/2}$. For $h \le 0.05$ the data fit a straight line well, so confirming the theoretical expectation.

It might be mentioned here that the amplitude $\bar{A}$ and limiting value $\Sigma(0)$ in (26) as well as the amplitudes in
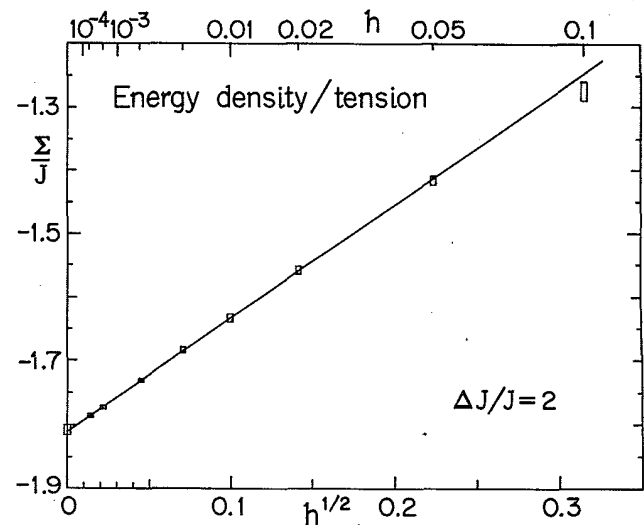

FIG. 6. Plot of the energy density or interfacial tension $\Sigma(h)$ induced by the random bonds vs $h^{1/2}$ for $\Delta J/J = 2$. Note the data for a free walk at $h = 0$. The straight line has an intercept $\Sigma(0)/J = -1.812$ and a slope 1.785.

(24) will depend on $\Delta J/J$ and should exhibit universal power-law behavior as $\Delta J \to 0$, the exponents being associated with the *crossover* to flat (or, for $T > 0$, pure thermal) behavior. This is an interesting topic for future study but we have not explored it so far.

In order to test the underlying scaling ansatz (3), which we may write quantitatively as

$$\bar{\xi}_\perp/b \approx (\xi_\parallel/a)^\zeta , \qquad (27)$$

one must calculate $\xi_\parallel(h)$. This is best done on the basis of the longitudinal correlation function

$$C_{av}(h;x,x',L_\parallel) \equiv \langle l_\omega(h;x,L_\parallel)l_\omega(h;x',L_\parallel) \rangle_\omega$$
$$- \langle l_\omega(h;x,L_\parallel) \rangle_\omega \langle l_\omega(h;x',L_\parallel) \rangle_\omega . \qquad (28)$$

Provided both x and x' remain within the region X_{eq}, one observes, as expected, that C depends only on h and the difference $|x - x'|$. Accordingly we estimate the true asymptotic correlation function from the average

$$C(h;x) \cong \langle C_{av}(h;x', x'+x, L_\parallel) \rangle_{eq} \qquad (29)$$

as for $\bar{l}(h)$.

The variation of the correlation function with x for various values of h is shown in Fig. 7. Evidently the decay becomes very slow for small h. To define the correlation length we use the second moment of $C(h;x)$ via

$$\xi_\parallel^2(h) \equiv \tfrac{1}{2}\int_0^\infty C(h;x)x^2\,dx \bigg/ \int_0^\infty C(h;x)\,dx . \qquad (30)$$

This definition, in addition to being sanctioned by large usage, pertains directly to scattering measurements at low momentum transfer. In fact, we tried definitions using other moments but found that the second seemed to balance the contributions of $C(x)$ at large and small x most reasonably. Note that if $C(x)$ had the precise form $C_0 \exp(-x/\xi_\parallel^0)$ then (30) would yield $\xi_\parallel = \xi_\parallel^0$. Indeed, the observed decay is, after a small initial "transient" fairly

close to exponential so one can roughly estimate $\xi_\parallel$ directly from a plot of $\log C(x)$ versus x. However, (30) provides a more systematic and reliable approach.

A practical effect that must be allowed for arises from the statistical fluctuations in $C(x)$ at large x which, clearly, preclude a smooth decay to zero. Since the fluctuations are weighted by x^2 they can lead to significant errors. Accordingly, we introduced a cutoff x_c on both integrals in (30). Then x_c was varied between the values x_1 and x_2 over which the plot of $\log C(x)$ was seen to be close to linear; beyond x_2 strong departures from this behavior signal the effects of statistical noise. In evaluating the integrals for $x > x_c$, a linear extrapolation of the linear region of the $\log C(x)$ plot was used. Thus for each value of x_c in (x_1, x_2) a value for $\xi_\parallel^2$ was obtained; averaging over these produces a reliable overall estimate. The uncertainties were judged as for $\bar{l}(h)$, etc., and amounted to about 2%.

The data obtained for $\xi_\parallel(h)$ are shown on a log-log plot versus $\xi_\perp(h)$ and $\bar{\xi}_{1e}(h)$ in Fig. 8; the open rectangles indicate the uncertainties. A least-squares fit for $\xi_\perp$ yields

$$\zeta = 0.655 \pm 0.014 , \qquad (31)$$

and this is confirmed by the technique used in Fig. 5. The data for $\bar{\xi}_{1e}$, analyzed along the same lines, suggest the slightly higher value $\zeta = 0.665 \pm 0.015$. Evidently the results are fully consistent with the theoretical expectation[1,2,6,7] $\zeta = \tfrac{2}{3}$.

If the theoretical prediction is accepted one finds, in (27),

$$b/a = 0.662 \pm 0.001 \qquad (32)$$

for $\Delta J/J = 2$; note, however, that b must depend strongly on $\Delta J/J$ and should, like the other nonuniversal amplitudes, display singular behavior as $\Delta J \to 0$. Data computed for *larger* values of ΔJ, ranging up to $\Delta J/J = 15$, at fixed h ($= 0.1$) can be fit roughly by $b^2 \simeq c_0[(\Delta J/J) - c_1]$ with $c_0 = 0.34$ and $c_1 = 0.67$. One observes that most of
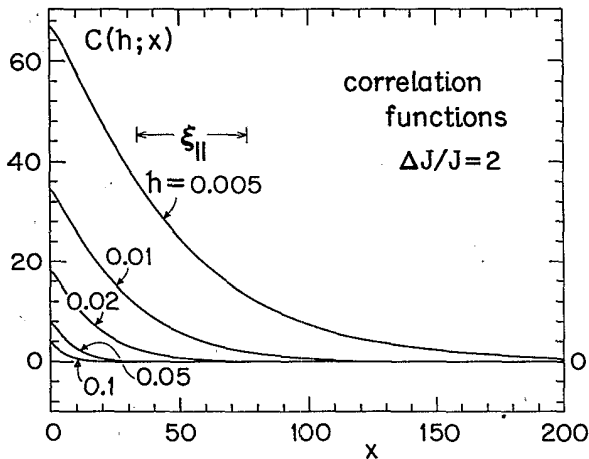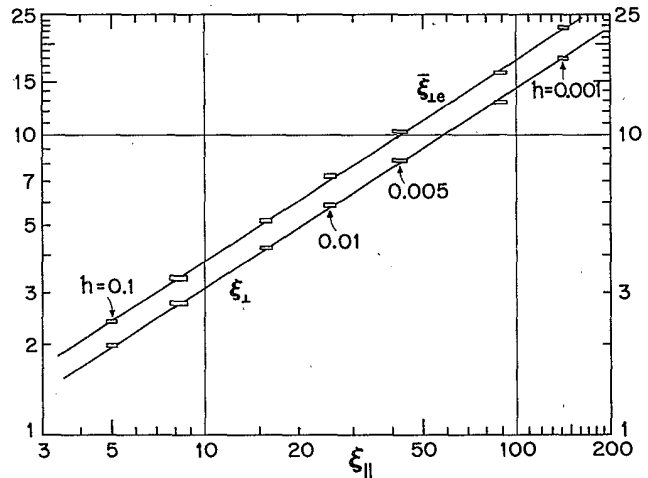
FIG. 7. Plots of the correlation functions $C(h;x)$ for various fields h with $\Delta J/J = 2$. The intercept $C(h;0)$ is equal to $\xi_\parallel^2(h)$. The double arrow measures $\xi_\parallel$ for $h = 0.005$.

FIG. 8. Tests of the basic fluctuation scaling hypothesis via logarithmic plots of $\xi_\perp$ and $\bar{\xi}_{1e}$ vs $\xi_\parallel$ for h from 0.1 to 0.001 (see some values marked on the graph) for $\Delta J/J = 2$. The straight lines have the predicted slope $\zeta = \tfrac{2}{3}$.

the variations arise from changes in $\xi_\perp(h)$; the value of $\xi_\parallel(h)$ drops only some 6 or 7 % as ΔJ increases. A little reflection indicates that this is not very surprising.

IV. SUMMARY

In conclusion, our numerical studies have served to confirm in detail for $d=2$ dimensions the scaling theory of complete wetting in a random medium developed by Lipowsky and Fisher.[1,2] Furthermore, a number of universal amplitude ratios, not predicted by scaling alone, have been evaluated [see (25)]. An interesting issue left unexplored concerns the behavior of various *nonuniversal* amplitudes, for the wetting layer thickness $\bar{l}(h)$, and the correlation lengths $\xi_\perp(h)$ and $\xi_\parallel(h)$, etc., in the weakly random limit $\Delta J/J \to 0$.

APPENDIX: TRANSFER-MATRIX ALGORITHMS

In this appendix we describe the method used by Huse and Henley[11] to calculate numerically the ground-state energy $E_\omega(x_1,z_1;x_2,z_2)$ of an interface or path running from (x_1,z_1) to (x_2,z_2) for an Ising square lattice of size $L_\parallel \times \Delta z$ under a given realization ω of all random bonds. For simplicity we restrict the presentation to the situa-

tion in which $J_\parallel = J$ is constant, as adopted in the practical calculations. However, it is easy to generalize the procedure to the case where $J_\parallel$ is a random but still positive variable (i.e., for random ferromagnetic couplings). Likewise we take $(x_1,z_1)=(0,0)$ and write $E_\omega(0,0;x,z) \equiv E(x,z)$.

The ground-state energy and the optimal path can clearly be calculated iteratively from

$$E(x+1,z) = \min_{z'}[E(x,z')+J|z'-z|]+\tilde{J}(x+1,z) ,$$

(A1)

where $\tilde{J}(x,z)=J_\perp(x,z)+Hz$. The basic manipulation is thus to transfer the set of values $E(x,z)$ for $0 < z \leq \Delta z$ to the set $E(x+1,z)$. A simple-minded method would take $(\Delta z)^2$ operations to do this, each operation being composed of computing $E(x,z')+J|z'-z|$ once and making Δz comparisons. The method explained here, which was used by Huse and Henley in their paper,[6] takes only $2\Delta z$ operations, thus substantially reducing the computational effort.

To start, focus on the first term on the right-hand side of (A1) and write it as

$$E'(x+1,z) \equiv \min_{z'}[E(x,z')+J|z'-z|]$$
$$=E(x+1,z)-\tilde{J}(x+1,z) . \quad (A2)$$

It is also helpful to define the *restricted* minimal energy

$$E''(x+1,z) = \min_{z'\leq z}[E(x,z')+J|z'-z|] . \quad (A3)$$

Then a crucial relation is

$$E'(x+1,z)=P(x,z) \equiv \min_{z'\geq z}[E''(x+1,z')+J|z'-z|] , \quad (A4)$$

which can be proved as follows:

$$P(x,z)= \min_{z'\geq z} \min_{z''\leq z'}\{[E(x,z'')+J|z''-z'|]+J|z'-z|\} = \min_{z''}\{\min_{z'\geq z'',z}[E(x,z'')+J|z''-z'|]+J|z'-z|\}$$

$$= \min_{z''}[E(x,z'')+J|z''-z|]=E'(x+1,z) . \quad (A5)$$

Now both $E''(x+1,z)$ and $E'(x+1,z)$ can be calculated iteratively by simple twofold comparisons since one has

$$E''(x+1,z+1)=Q(x,z) \equiv \min\{E(x,z+1);E''(x+1,z)+J\} , \quad (A6)$$

$$E'(x+1,z)=\min\{E''(x+1,z);E'(x+1,z+1)+J\} . \quad (A7)$$

These relations are easily proved; thus by (A3) one has

$$E''(x+1,z+1) \equiv \min_{z'\leq z+1}[E(x,z')+J|z'-(z+1)|]=\min\{E(x,z+1); \min_{z'\leq z}[E(x,z')+J|z'-(z+1)|]\}=Q(x,z) . \quad (A8)$$

A similar argument gives (A7). Finally one obtains $E(x+1,z)$ from $E'(x+1,z)$ by using (A1). Note that (A6) and (A7) show that the total number of operations needed to effect the transfer from x to $x+1$ is just $2\Delta z$.

[1]R. Lipowsky and M. E. Fisher, Phys. Rev. Lett. **56**, 472 (1986).
[2]M. E. Fisher, J. Chem. Soc. Faraday Trans. 2 **82**, 1569 (1986) (Faraday Symp. 20).
[3]G. Grinstein and S.-K. Ma, Phys. Rev. B **28**, 2588 (1983).
[4]J. Villain, J. Phys. (Paris) **43**, L551 (1982).
[5]T. Natterman, J. Phys. C **16**, 4113 (1983).
[6]D. A. Huse and C. L. Henley, Phys. Rev. Lett. **54**, 2708 (1985).
[7]D. A. Huse, C. L. Henley, and D. S. Fisher, Phys. Rev. Lett.

55, 2924 (1985).

[8]See, e.g., D. A. Huse, W. Van Saarloos, and J. D. Weeks, Phys. Rev. B **32**, 233 (1985).

[9]B. Derrida and J. Vannimenus, Phys. Rev. B **27**, 4401 (1983).

[10]W. H. Press, B. P. Flannery, S. A. Teukolsky, and W. T. Vetterling, *Numerical Recipes: The Art of Scientific Computing* (Cambridge University Press, New York, 1986), Chap. 7, p. 196.

[11]D. A. Huse and C. L. Henley (private communication).